

# Development of a CP $^{31}\text{P}$ NMR Broadline Simulation Methodology for Studying the Interactions of Antihypertensive $\text{AT}_1$ Antagonist Losartan with Phospholipid Bilayers

Charalambos Fotakis,<sup>†</sup> Dionisios Christodouleas,<sup>†</sup> Petros Chatzigeorgiou,<sup>†</sup> Maria Zervou,<sup>‡</sup> Nikolas-Ploutarch Benetis,<sup>‡</sup> Kyriakos Viras,<sup>†</sup> and Thomas Mavromoustakos<sup>†\*</sup>

<sup>†</sup>Chemistry Department, University of Athens, Athens, Greece; and <sup>‡</sup>National Hellenic Research Foundation, Institute of Organic and Pharmaceutical Chemistry, Athens, Greece

**ABSTRACT** A cross-polarization (CP)  $^{31}\text{P}$  NMR broadline simulation methodology was developed for studying the effects of drugs in phospholipids bilayers. Based on seven-parameter fittings, this methodology provided information concerning the conformational changes and dynamics effects of losartan in the polar region of the dipalmitoylphosphatidylcholine bilayers. The test molecule for this study was losartan, an antihypertensive drug known to exert its effect on  $\text{AT}_1$  transmembrane receptors. The results were complemented and compared with those of differential scanning calorimetry, solid-state  $^{13}\text{C}$  NMR spectroscopy, Raman spectroscopy, and electron spin resonance. More specifically, these physical chemical methodologies indicated that the amphipathic losartan molecule interacts with the hydrophilic-head zone of the lipid bilayers. The CP  $^{31}\text{P}$  NMR broadline simulations showed that the lipid molecules in the bilayers containing losartan displayed greater collective tilt compared to the tilt displayed by the load-free bilayers, indicating improved packing. The Raman results displayed a decrease in the *trans/gauche* ratio and increased intermolecular interactions of the acyl chains in the liquid crystalline phase. Additional evidence, suggesting that losartan possibly anchors in the realm of the headgroup, was derived from upfield shift of the average chemical shift  $\sigma^{\text{iso}}$  of the  $^{31}\text{P}$  signal in the presence of losartan and from shift of the observed peak at  $715\text{ cm}^{-1}$  attributed to C-N stretching in the Raman spectra.

## INTRODUCTION

Hypertension can create extensive medical challenges, and it can cause an increased risk for dangerous medical conditions such as heart disease leading to a heart attack. Although the exact mechanism of the molecular basis of hypertension is still unknown, it has been postulated that cell membranes play an important role in its cause and progression. Our laboratory has been involved in the exploration of the conformational properties of commercially available sartans and synthetic derivatives in an attempt to elaborate on the role of the conformation in the favor binding at the  $\text{AT}_1$  receptor (1–6).

In the study presented here, a methodology of broadline cross-polarization (CP)  $^{31}\text{P}$  NMR simulations has been developed. A simplified dynamical model was used with the studied dipalmitoyl phosphatidyl choline (DPPC) multilamellar bilayers considered to be immobilized in the time-scale of the NMR experiment, whereas the lipid molecules were assumed to perform fast overall rotational diffusion in both the liquid crystalline and in the more organized gel phase. A detailed theory of the broadline CP  $^{31}\text{P}$  NMR simulations of fully hydrated DPPC dispersions in the form of lipid bilayers was published earlier (7). In this work, an automated fitting method using seven parameters was used to enhance the performance of the CP  $^{31}\text{P}$  NMR spectral simulations.

In general, phosphatidyl choline bilayers exist in the gel phase ( $L_\beta$ ) at low temperatures and in the liquid crystalline phase ( $L_\alpha$ ) at higher temperatures. The liquid crystalline phase and the gel phase are known to exhibit long-range orientation order, whereas the gel phase possesses, additionally, long-range translational order. These properties are intimately related to the concept of the packing quality of the lipids in the bilayer. Overall uniaxial rotation, fluctuations, or wobbling of the axis of rotation (8); internal rotations (9); and lateral diffusion within the plane of the bilayer (10,11) are motions of the lipid molecules subjected to restrictions posed by the anisotropic environment of the bilayer. The transition from gel to liquid crystalline is accompanied by several structural changes in the lipid molecules, as well as by systematic alteration in the bilayer geometry. The most prominent feature, however, is the *trans/gauche* isomerization taking place in the acyl conformation. The average number of *gauche* conformers indicates the effective fluidity, which depends not only on the temperature, but also on perturbations due to the presence of a drug molecule intercalating between the lipids.

In our studies, DPPC bilayers were chosen as the model membrane, because their mesomorphic changes occur in a convenient temperature range and their physical and chemical properties have been well studied (11,12). Losartan was chosen as the test molecule (Fig. 1), because it is a well-known bioactive molecule that produces beneficial effects in the treatment of hypertension (13). Losartan is the first marketed antihypertensive drug, designed to mimic the

Submitted June 15, 2008, and accepted for publication November 20, 2008.

\*Correspondence: tmavro@cie.gr

Editor: Mark Girvin.

© 2009 by the Biophysical Society  
0006-3495/09/03/2227/10 \$2.00

doi: 10.1016/j.bpj.2008.11.057

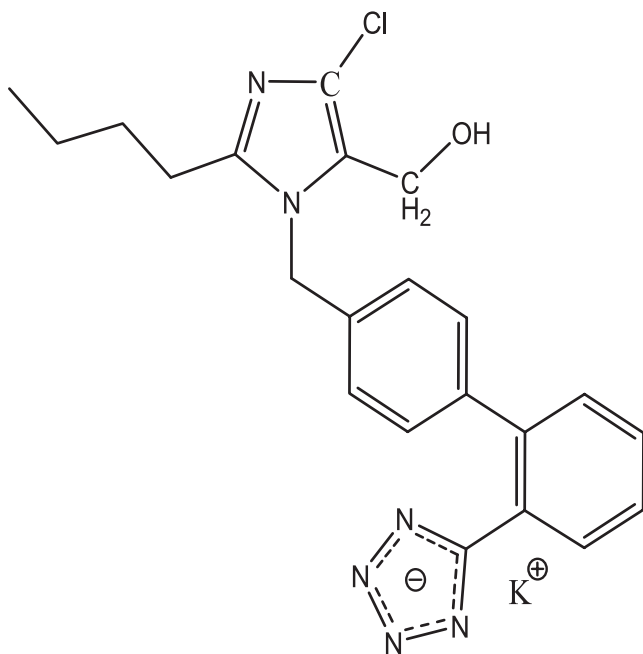


FIGURE 1 Molecular structure of losartan .

C-terminal segment of angiotensin II and to selectively hinder its effect at the active site of the AT<sub>1</sub> receptor (14). Our laboratory has proposed a two-step mechanism in which this antihypertensive AT<sub>1</sub> antagonist is first incorporated into the bilayer through the lipid-water interface and then laterally diffuses to reach the active site of the AT<sub>1</sub> receptor (15).

The interactions of losartan with the DPPC membrane were studied. The effects of losartan in lipid bilayers have been studied previously by using differential scanning calorimetry (DSC) and solid-state high-resolution <sup>13</sup>C MAS NMR spectroscopy. The published results showed that losartan causes lowering of the main phase transition temperature in the hosting fully hydrated DPPC bilayers in a concentration-dependent manner and that, from molar ratio equal to 5% and higher, it abolishes pretransition (16). <sup>13</sup>C MAS NMR and electron spin resonance data showed that losartan decreased the chain mobility of DPPC bilayers in both the gel and the liquid crystalline phases. Molecular modeling calculations, in agreement with DSC, <sup>13</sup>C MAS NMR, and electron spin resonance data, suggested that the favorable location of losartan was in the realm of the phosphate group (15,17). To gain insight into the conformational changes and dynamic effects that losartan induces on the lipid bilayers, static CP <sup>31</sup>P as well as Raman spectroscopy were applied in the temperature range covering all mesomorphic states of lipid bilayers, in the absence or presence of incorporated losartan. To our knowledge, this is the first study of solid-state <sup>31</sup>P NMR spectroscopy with this aim. The results derived are in agreement with those obtained by DSC, solid-state high-resolution <sup>13</sup>C NMR, and Raman spectroscopy. The comparison of the results of the developed methodology with the results of the above established methods in this field indicates that the

new method can provide valuable information on issues related to drug/cell membrane interactions.

## METHODS

L $\alpha$ -DPPC (99+%) was purchased from Avanti Polar Lipids (Alabaster, AL), and spectroscopic grade CHCl<sub>3</sub> was obtained from Sigma Aldrich (St. Louis, MO). Losartan was kindly donated by Merck (Whitehouse Station, NJ).

Appropriate amounts of DPPC with or without losartan were dissolved in spectroscopic grade chloroform. The solvent was then evaporated by passing a stream of O<sub>2</sub>-free nitrogen over the solution at 50°C, and the residue was placed in a vacuum (0.1 mm Hg) for 24 h. To obtain measurements, this dry residue was dispersed in appropriate amounts of bidistilled water by vortexing. The lipid content for the three samples used in the stationary <sup>31</sup>P NMR experiments was ~40 mg, and water was dispersed within it (50% w/w). The DPPC/losartan bilayers contained a 20% mol ratio of drug. The DPPC bilayer's <sup>31</sup>P resonance was referenced to an H<sub>2</sub>PO<sub>4</sub> 85% chemical shift and also compared with results stated in relevant literature (18).

Static <sup>31</sup>P NMR, proton CP spectra were obtained on a Bruker (Karlsruhe, Germany) MSL 400 NMR spectrometer operating at 161.977 MHz and capable of high-power <sup>1</sup>H-decoupling. Each spectrum was an accumulation of 1000 scans. The standard pulse sequence of the Bruker software for the CP experiment was used with the following acquisition parameters: recycling delay 4 s, contact time 5 ms, acquisition time 1 ms,  $\pi/2$  pulse for proton 7  $\mu$ s. The contact time was chosen to give optimal spectra after testing at 1, 3, and 5 ms. The temperature range used in the experiments was 25–50°C. The sample was revolved in a 4-mM rotor at a low frequency of 25 Hz.

Another portion of the prepared sample (~40 mg) was used for the Raman spectroscopy experiments. The Raman spectra were obtained at 4 cm<sup>-1</sup> resolution from 3500–400 cm<sup>-1</sup> with interval 2 cm<sup>-1</sup> using a Perkin-Elmer (Shelton, CT) NIR FT-spectrometer (Spectrum GX II) equipped with a charge-coupled device detector. The measurements were performed at a temperature range of 27–50°C. The laser power (a Nd:YAG at 1064 nm) was kept constant at 400 mW during the experiments. Fifteen hundred scans were accumulated, and back-scattering light was collected.

All the simulations were obtained imposing Lorentzian spin packets, and the experimental spectra were performed by automated fitting using the downhill simplex algorithm. This version of the simplex optimization (19) was implemented in this work after appropriate modifications of the original Fortran code. In the presented fitting procedure, the residual sum of squares,  $RSS = \sum_i (y_{i;experim} - y_{i;comput})^2$ , was minimized by the downhill simplex to a convergence criterion from 0.05 to 0.01. The indexed  $y_i$  values represent the normalized to the maximum intensity of the spectra at the point  $i$ .

## RESULTS AND DISCUSSION

### Spectral simulations of <sup>31</sup>P NMR broadlines

The spectra simulated in this study were referred to fully hydrated phospholipid bilayers of DPPC in the absence or presence of incorporated losartan (7,20). The combination of three effects—the uniaxial rotation of the lipid molecules around the long axis, the restoring potential of the lamellar structures of the bilayers by the field, and the differential cross-polarization of the differently oriented spin packets—gives simulated lines that are very similar to the experimental broadlines, as the convergence criterion implies. The variation of spectra simulation parameters versus temperature is shown in Tables 1 and 2. Temperature profiles of the drug-free and losartan-loaded bilayers versus selective parameters were plotted in the same diagram and compared with each

**TABLE 1** Spectral simulations parameters for CP <sup>31</sup>P NMR spectra of the DPPC bilayers in the temperature range 25–50°C

T/°C	brd/ppm	CS-tensor/ppm	( $\alpha, \beta$ )°	$\sigma_{\text{iso}}$	$\Delta\sigma$ /ppm	eCPE	$\vartheta_{\text{DR}}$	$V_0/K$
25	6.61	(−94.21, −33.22, 95.78)	(22.66, 38.23)	−10.55	55.70	0.642	24.64	1.24E-02
27	6.83	(−93.69, −33.69, 95.30)	(26.44, 38.69)	−10.69	55.17	0.702	29.20	2.74E-02
30	5.34	(−94.61, −34.62, 94.38)	(24.48, 40.21)	−11.61	47.26	0.867	19.09	2.67E-02
32	3.74	(−94.71, −34.71, 94.29)	(25.67, 41.46)	−11.71	42.12	0.864	20.53	1.12E-02
33	3.32	(−95.28, −35.28, 93.72)	(25.64, 41.57)	−12.28	41.60	0.912	16.31	1.13E-02
35	2.66	(−95.27, −35.27, 93.73)	(22.71, 41.30)	−12.27	41.34	1.034	9.32	2.39E-02
36	2.50	(−95.08, −35.08, 93.92)	(24.59, 41.32)	−12.08	42.21	1.047	15.82	2.12E-02
38	2.24	(−95.14, −35.14, 93.84)	(28.64, 40.87)	−12.15	41.55	1.104	3.82	3.62E-02
40	1.99	(−94.89, −34.89, 94.09)	(24.11, 41.45)	−11.90	41.36	1.062	2.17	3.59E-02
42	2.39	(−95.03, −35.03, 93.95)	(14.80, 40.66)	−12.03	41.12	1.077	2.78	4.39E-02
43	2.30	(−95.03, −35.03, 93.95)	(12.85, 40.54)	−12.03	41.10	1.070	4.39	4.75E-02
45	2.65	(−94.58, −34.58, 94.40)	(15.89, 40.61)	−11.59	41.75	1.112	10.11	4.40E-02
46	2.28	(−94.62, −34.62, 94.36)	(13.93, 40.49)	−11.62	41.65	1.061	10.24	4.60E-02
47	2.09	(−94.55, −34.55, 94.43)	(9.537, 40.16)	−11.56	42.11	1.061	11.22	4.74E-02
49	2.29	(−94.87, −34.87, 94.11)	(8.152, 40.08)	−11.88	42.24	1.129	12.16	2.95E-02
50	2.06	(−94.76, −34.76, 94.22)	(4.338, 40.27)	−11.76	40.74	1.070	11.51	4.39E-02

other. In these profiles, information regarding the dynamical and indirectly conformational characteristics of the bilayers alone or with incorporated losartan was extracted.

### Chemical shielding tensor $\sigma$

The effectively axial chemical shielding (CS) tensor component  $\sigma_{zz}^{\text{aniso}}$  is first computed by the relation,

$$\sigma_{zz}^{\text{aniso}}(\alpha, \beta) = \frac{1}{2} \left\{ (\sigma_{zz} - \sigma_{\text{iso}}) (3\cos^2\beta - 1) + (\sigma_{xx} - \sigma_{yy}) \cos 2\alpha \sin^2\beta \right\}, \quad (1)$$

where the polar angles ( $\alpha, \beta$ ) determine the orientation of the rotation axis in the CS tensor principal frame (7). This relation was obtained by keeping only the secular part of the Zeeman interaction and considering only overall molecular rotation (7). A more elaborate theory also involving internal rotations was given by Kohler and Klein (9). The average shift and the inhomogeneous broadening residual anisotropy (21) of the <sup>31</sup>P broadlines is determined by the components

$\sigma_{xx}, \sigma_{yy}, \sigma_{zz}$ . The computation of these measurables can be performed using Eq. 1.

Experimental results obtained at very low temperatures (250 K and lower) have indicated that the rotational motion of the lipid molecules around their long axis and/or internal rotations cease (12) and that the configuration of the phosphate in phospholipids leads in general to a rhombic CS tensor. At higher temperatures, the fast uniaxial rotation of the lipid molecules around their long axis results in the partial averaging of the CS tensor. This motion transforms the rhombic CS tensor of the P-31 to an effectively axial tensor with axis of highest symmetry, the axis of the rotation (Fig. 2). By the same motion, this axis of symmetry is shared also by an effectively axial dipolar interaction of the <sup>31</sup>P nucleus with the nearest protons. The direction of the rotation axis inside the bilayer is considered to be arbitrary, depending on the temperature and the presence of the drug.

The variable  $\sigma_{zz}^{\text{aniso}}$  is further used for the construction of the powder lineshape as if the chemical shielding tensor was axial. Axial tensors give powder lineshapes characterized by

**TABLE 2** Spectral simulations parameters for CP <sup>31</sup>P NMR spectra of the DPPC/losartan bilayers in the temperature range 25–50°C

T/°C	brd/ppm	CS-tensor/ppm	( $\alpha, \beta$ )°	$\sigma_{\text{iso}}$	$\Delta\sigma$ /ppm	eCPE	$\vartheta_{\text{DR}}$	$V_0/K$
25	8.10	(−102.6, −43.55, 86.45)	(41.37, 41.27)	−19.91	52.99	0.68	34.10	2.95E-02
27	7.34	(−102.3, −43.22, 86.78)	(44.45, 41.39)	−19.57	54.56	0.64	35.87	3.03E-02
30	6.85	(−102.1, −43.04, 86.96)	(42.20, 40.72)	−19.40	55.85	0.57	38.00	3.03E-02
32	5.98	(−102.6, −43.53, 86.47)	(39.83, 40.21)	−19.89	56.47	0.43	31.96	2.88E-02
33	6.06	(−103.1, −44.02, 85.98)	(37.35, 40.08)	−20.37	55.46	0.38	30.05	2.35E-02
35	5.58	(−104.0, −44.94, 85.06)	(17.42, 38.13)	−21.27	54.44	0.26	17.61	1.20E-02
36	5.32	(−104.5, −45.52, 84.48)	(17.38, 38.55)	−21.85	52.09	0.28	14.06	1.30E-02
38	4.91	(−104.2, −45.21, 84.79)	(17.55, 38.64)	−21.55	52.09	0.31	13.53	1.22E-02
40	4.40	(−104.6, −45.54, 84.46)	(19.55, 38.81)	−21.88	52.01	0.27	12.76	1.03E-02
42	4.11	(−104.4, −45.36, 84.64)	(17.68, 38.82)	−21.69	51.28	0.41	11.02	1.25E-02
43	4.21	(−104.1, −45.07, 84.93)	(16.79, 39.03)	−21.42	49.99	0.50	17.48	1.25E-02
45	3.85	(−104.3, −45.34, 84.66)	(17.64, 39.64)	−21.67	47.41	0.60	18.55	2.27E-02
46	3.46	(−104.2, −45.20, 84.80)	(16.04, 39.90)	−21.55	45.62	0.61	16.81	2.08E-02
47	3.31	(−104.1, −45.08, 84.92)	(16.14, 40.24)	−21.43	44.03	0.62	14.11	2.01E-02
49	2.72	(−104.4, −45.35, 84.65)	(16.52, 40.57)	−21.69	42.62	0.66	14.50	2.43E-02
50	2.54	(−104.4, −45.36, 84.64)	(9.950, 40.26)	−21.70	42.18	0.52	15.17	2.64E-02

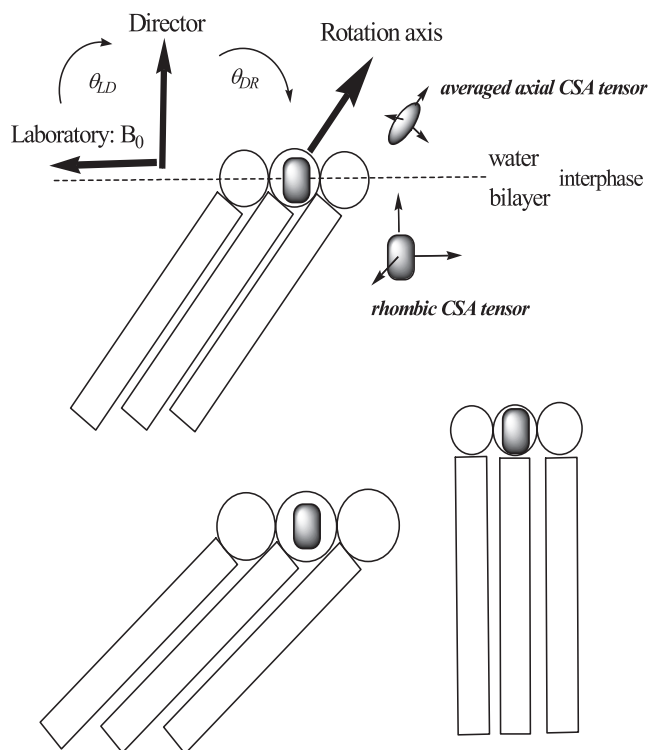


FIGURE 2 Overall view of the entire model system revealing the basic geometrical parameters such as the angle  $\theta_{DR}$  between the director and the rotation axis. (Lower panels) Impact of the dimensions of the headgroup on the collective tilt and on the bilayer order: lower left, voluminous headgroup (e.g., phosphatidylcholine); lower right, small headgroup (e.g., phosphatidylethanolamine).

two distinctively unequal discontinuities shown as uneven peaks at the edges of the broadline, as was also demonstrated by the experimental broadlines obtained in this work (Figs. 3 and 4).

In our study, an increase in the azimuthal angle  $a$  corresponds to an increase of the inhomogeneous broadening  $\Delta\sigma = 3\sigma_z^{\text{anis}}/2$ . The opposite trend was observed for the variation of the polar angle  $\beta$ , i.e.,  $\beta$  and  $\Delta\sigma$  are inversely proportional. The above trends depend on the particular values of the principal CS tensor components and their orientation with respect to the long axis of the DPPC molecule (Fig. 5).

The values, found in the literature, of  $\sigma = (-81, -21, 108)$  ppm for the components of the  $^{31}\text{P}$  CS tensor of general rhombic symmetry were adopted as initial values in the fitting procedure of the lineshape simulations in this study. This tensor has been obtained experimentally at 163 K in water dispersions of 50% DPPC: water by weight, with 85% orthophosphoric acid used as reference (12).

The average chemical shift of the broadline, expressed as the trace  $\sigma^{\text{iso}} = (\sigma_{11} + \sigma_{22} + \sigma_{33})/3$  of the CS tensor, was first estimated. The value of the average chemical shift  $\sigma^{\text{iso}}$  remained practically constant around the value  $-11.9$  ppm for all the measurement temperatures of DPPC bilayers, displaying only rather weak temperature dependence (Table 1).

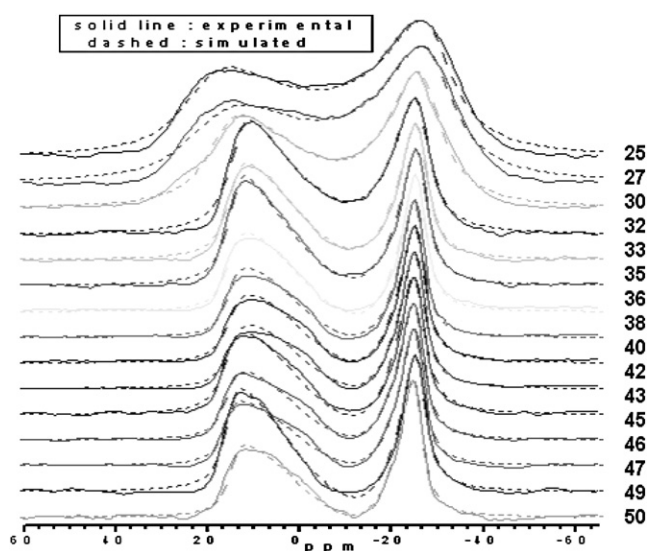


FIGURE 3 Experimental and simulated spectra of DPPC bilayers in the temperature range of 25–50°C.

When Losartan was added in the DPPC bilayers, the average chemical shift  $\sigma^{\text{iso}}$  of the  $^{31}\text{P}$  signal shifted upfield to an average of  $-21.7$  ppm (Tables 1 and 2). A plausible explanation for this significant change is that the tetrazole moiety of the drug is attached close to the choline group of the lipid in the hydrophilic zone of the bilayer, in the direct area of the lipid-water interface. Such an explanation is in agreement with the reported molecular modeling data (15).

The orientation of the rotation axis, i.e., the molecular long axis of the lipids specified by the azimuthal and the polar angles ( $\alpha, \beta$ ) in the principal CS-tensor frame (Fig. 6), is correlated with the orientation and the internal structure of the headgroup. The initial values  $(\alpha, \beta) = (20, 35)$  were adopted from our earlier publication concerning the DPPC

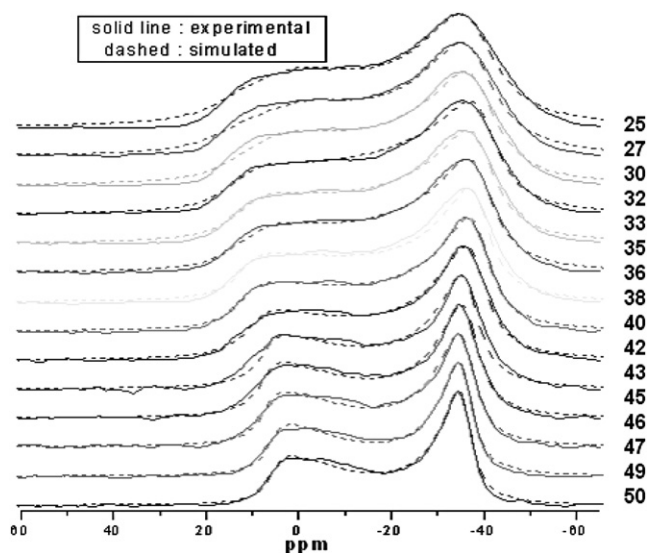


FIGURE 4 Experimental and simulated spectra of losartan-loaded DPPC bilayers in the temperature range of 25–50°C.



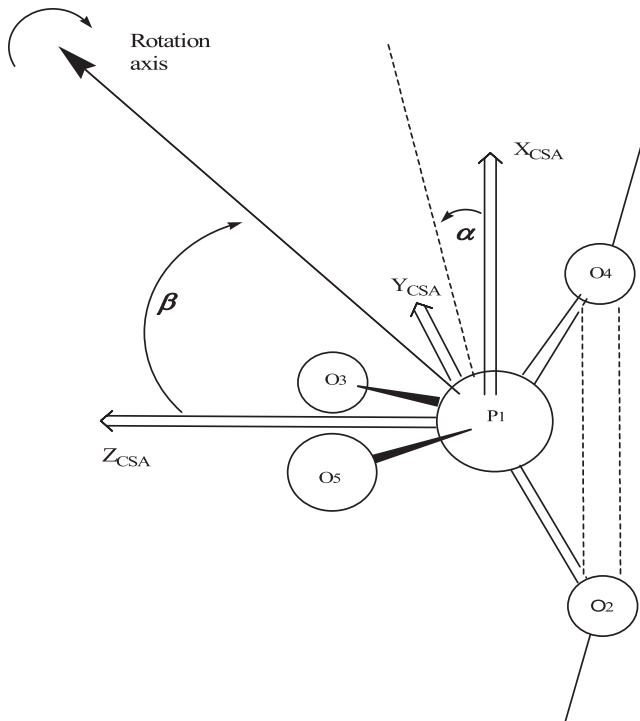


FIGURE 5 Structure of the phosphate fragment around the  $^{31}\text{P}$  atom and the relative orientation of the rotation axis with respect to the principal  $\sigma$ -tensor frame of the phosphate fragment.

bilayers with or without small peptides (7), and were further fitted during the spectral simulations of the presented systems. The main characteristic of the presented temperature profiles of DPPC bilayers is the significant change of the azimuthal angle  $\alpha = 23^\circ$  in the gel  $L_\beta$  phase to  $\alpha = 4^\circ$  in the liquid crystalline  $L_\alpha$  phase (Fig. 6). This is an indication of the change of the conformation/orientation of the headgroup accompanying the main phase transition. The

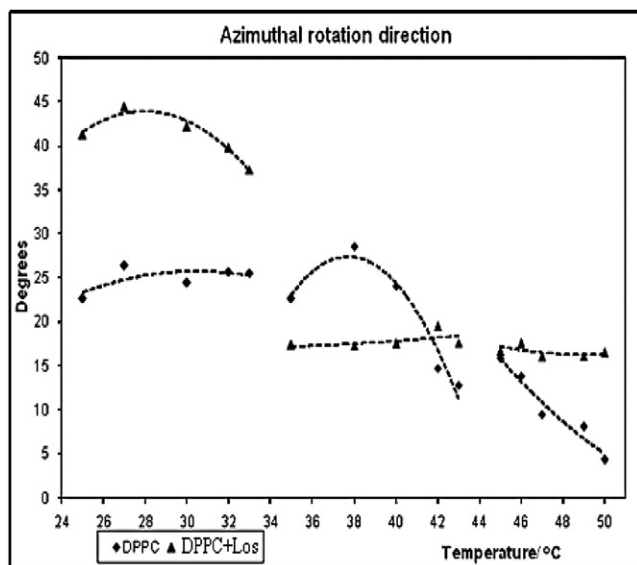


FIGURE 6 Temperature profile of the azimuthal angle  $\alpha$ .

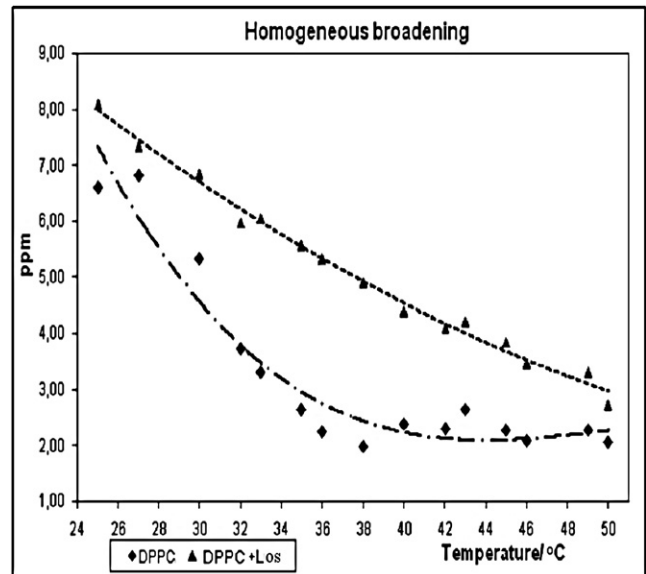


FIGURE 7 Temperature profiles of the homogeneous broadening parameter  $\text{brd}$  of the DPPC bilayers without and with losartan.

presence of losartan in DPPC bilayers causes a significant disturbance of the headgroup orientation, which is seen in the temperature profiles of Fig. 6 as a doubling of the azimuthal angle  $\alpha$  in the gel phase.

Importantly, the whole series of the temperature profiles of  $\sigma^{\text{iso}}$  were simulated with insignificant change to the three elements of the CS tensor (Table 1). This reinforces the validity of the presented theoretical model of the  $^{31}\text{P}$ -NMR simulations, according to which the values of the components of the CS tensor do not change significantly with the temperature.

### Intrinsic or homogeneous broadening of spin packets

This is the broadening imposed on each one of the superimposed spin packets, to give the  $^{31}\text{P}$  broadline. The main cause of the intrinsic broadening here is the dipolar  $^1\text{H}$ - $^{31}\text{P}$  interaction of the phosphorous with the neighboring methylene protons and also to a minor extend, the CS-tensor anisotropy. The parameter that monitors the mobility of the individual lipid molecules will be referred to as  $\text{brd}$ ; greater broadening indicates decreased mobility but is only weakly correlated with the phase changes of the bilayers (7,20).

The  $\text{brd}$  (Fig. 7) decreases monotonically in a smooth fashion with increased temperature, as the mobility of the individual molecules increases. Thus, the modulation of the dipole-dipole and the CS anisotropy, which are responsible for the broadening of the spin-packet transitions, are almost independent of the phase transition of the bilayers, at least for the studied temperature range of 25–50°C (7,20). Furthermore, it was concluded that the lipid molecules in the losartan-loaded bilayers are less mobile than are those in

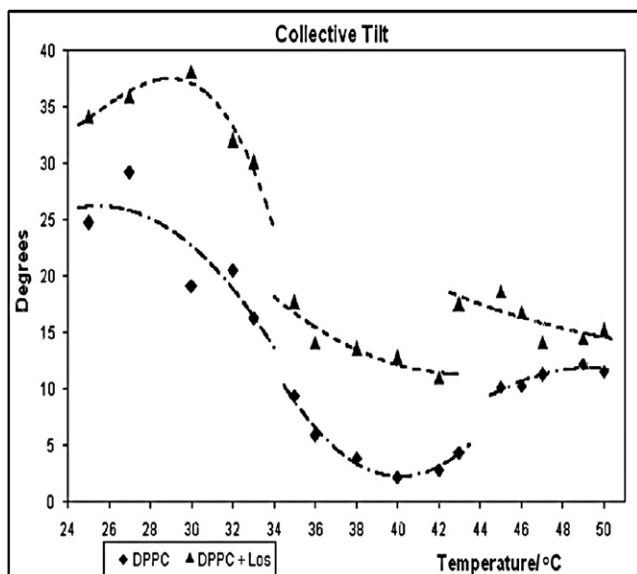


FIGURE 8 Temperature profiles of the collective tilt angle  $\vartheta_{DR}$  of the DPPC bilayers without and with losartan.

the losartan-free DPPC sample, because  $\text{brd}$  is greater in the losartan-loaded bilayers over the entire temperature range.

### Collective tilt angle $\vartheta_{DR}$

The average orientation of the lipid molecules with respect to the bilayer/membrane surface is specified by the angle  $\vartheta_{DR}$  between the director ( $D$ , the unit normal to the lamellae) and the long axis of the phospholipid molecules (Fig. 2). The angle  $\vartheta_{DR}$  refers to the collective tilt of the lipids and is related to the long-range orientational order of the bilayer. In particular, greatest collective tilt  $\vartheta_{DR}$  of the alkyl chain of the phospholipids is connected with increased order of the bilayer (22); thus,  $\vartheta_{DR}$  is an appropriate parameter for the determination of phase transitions.

In the temperature profiles of the angle  $\vartheta_{DR}$  (Fig. 8), it is shown that larger values of this angle occur in the gel phase, whereas the smaller values of this angle occur at higher temperatures. This is in agreement with the theoretical model proposed in this work and indicates the improved long-range orientational order of the lipids expected at lower temperatures. In addition, the collective tilt increases with the inclusion of losartan in the bilayers (10), and, therefore, it was concluded that the drug improves the organization of the bilayers compared to their organization free of drug. This is attributed to the fact that insertion of the losartan molecules in the hydrophilic headgroup zone increases the local volume of this zone, leading to a greater tilt of the lipid molecules.

The phase-transition temperatures are identified in the temperature profiles of the angle  $\vartheta_{DR}$  at temperatures around 35°C and 43°C, where sudden changes of the slope of the temperature profiles occur. The existence of three lamellar phases for pure DPPC bilayers and for DPPC/losartan bilayers could be concluded (Fig. 8). In particular, the larger

values of  $\vartheta_{DR}$  are observed in the range of 25–35°C, although the angle  $\vartheta_{DR}$  never exceeded 45°. This temperature interval coincides with the gel phase of the bilayer. From 35–43°C, the lowest values of  $\vartheta_{DR}$  are observed and the profile exhibits slight changes with increases temperature. This intermediate region appears to consist of lipids perpendicular in average to the lamellar surface. From 43–50°C an increase of  $\vartheta_{DR}$  is observed. This is opposite to the expected decreasing order of the bilayers with increasing temperature. A plausible explanation for this observation is that losartan as an amphiphilic drug is found to be localized at the interface that covers polar region and upper segment of the lipophilic region to maximize its amphipathic interactions. Such a localization of the drug induces a local curvature and opens the space between the adjacent alkyl chains. This could allow the tails of the alkyl chains of the next layer to entangle, introducing tail interdigitation. X ray diffraction results in progress are compatible with such an explanation. Such a tail interdigitation is expected to tighten the packing of the alkyl chain by maximizing van der Waals interactions (15,23–25).

### Restoring potential: curvature $V_0/K$

In this work, it is assumed that the external magnetic field exerts a weak torque, represented by a parabolic potential well with strength proportional to the curvature parameter  $V_0$ , measured in Kelvin. This torque tends to align the bilayer surface along with it. This particular orientative tendency is called negative ordering of the anisotropic magnetic susceptibility of the DPPC molecules (26). The parabolic potential possesses a single minimum at the angle of equilibrium  $\vartheta_{LD}$  between the direction of the magnetic field (laboratory,  $L$ ) and the local director (the normal to the lamellar surface) (Fig. 2). The appropriate value of the angle  $\vartheta_{LD}$  corresponding to negative ordering in the present case is 90° (5) and has been used by other investigators for producing aligned lamellar samples of lipids (27).

### Inhomogeneous broadening or residual anisotropy $\Delta\sigma/\text{ppm}$

The corresponding variable  $\Delta\sigma = 3 \sigma_z^{\text{anis}}/2$  obtained by the anisotropic part of the CS tensor, according to Eq. 1, determines the inhomogeneous broadening (residual anisotropy). The total width of the experimental  $^{31}\text{P}$  NMR spectra is a result of the anisotropic Zeeman interaction of the phosphorous magnetic moment and the random orientation of the bilayers in the sample. This variable is related to the internal structure and the orientation of the hydrophilic headgroup and is strongly phase dependent. In particular,  $\Delta\sigma$  is related to the collective properties of the membranes and depends on the orientation of the rotation axis with respect to the principal frame of the CS tensor (Fig. 5). Furthermore, because of the large (algebraic) difference of the parallel  $\sigma_{zz}$  and the average perpendicular component  $\sigma_{\perp} = (\sigma_{xx} + \sigma_{yy})/2$  of the CS

tensor, the inhomogeneous broadening is much more sensitive to the variation of the angle  $\beta$ .

In the temperature profile of  $\Delta\sigma$  (Fig. 9), the existence of sudden changes in the slopes around 33°C and 43°C suggest that three phases occur. This is in agreement with the profile of the azimuthal angle  $\alpha$  in Fig. 5 and of the collective tilt in Fig. 8. The presence of the drug makes the transitions less steep in accordance with published DSC results (15). At a temperature range of 25–30°C and 48–50°C, DPPC bilayers with and without losartan show similar  $\Delta\sigma$  values. Between the temperature range of 35–45°C, significant deviations to the  $\Delta\sigma$  values between the two samples are observed. This indicates a change in the internal structure and the orientation of the hydrophilic headgroup in the DPPC bilayers.

### The CP enhancement parameter eCPE

In the presented NMR broadline simulations, the effective enhancement of the  $^{31}\text{P}$  signal was represented by a single empirical parameter eCPE. The spin dynamics leading to CP were not examined thoroughly, with the focus mostly on the motional dynamics and the effects of the anisotropy of the bilayer on the lineshape. The dipolar interaction of the  $^{31}\text{P}$  nucleus coupled to the neighboring alkyl protons results in CP enhancing of the phosphorous signal. The accumulated effect of the four closest ethylene protons on the phosphorous nucleus can be represented by an equivalent overall axial dipolar tensor that enhances the phosphorous signal. In fact, the highest symmetry axes of the dipolar and the CS tensor must coincide, because they are both axially averaged by the overall rotation of the lipids about their long axes. The empirical parameter eCPE employed in the presented simulation model thus determines the overall efficiency of the cross-polarization.

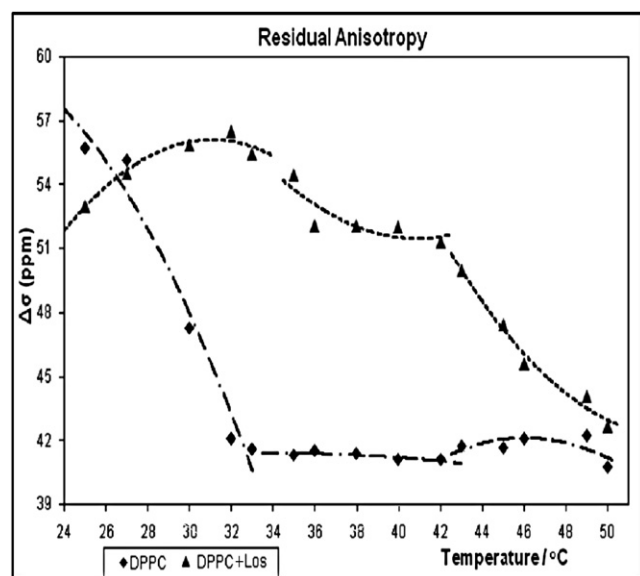


FIGURE 9 Temperature profiles of the inhomogeneous broadening (residual anisotropy  $\Delta\sigma$ ) of the DPPC bilayers without and with losartan.

As is shown in Figs. 3 and 4, an increased value of eCPE was observed with increasing temperature, rendering a more pronounced dip of the broadline with center at the spin packet corresponding to an angle of the lipid equal to the magic angle of 54.74°.

### Restrictions of the simulation parameters

The first restriction imposed by the theoretical model was setting  $\vartheta_{\text{LD}}$ , the angle between the static field and the director, to 90°, which is valid for the particular samples of the phospholipids. This was due to the negative ordering of the lipid bilayers restricting the fluctuations of the lamellar surface to occur around the direction of the field.

It is inferred that some of the fitted parameters in the simulation model are mutually correlated. The most obvious example is the “freedom” of using different components ( $\sigma_{xx}$ ,  $\sigma_{yy}$ ,  $\sigma_{zz}$ ) and orientation ( $\alpha$ ,  $\beta$ ) of the rotation axis with respect to the CS tensor, to fit the same isotropic chemical shift  $\sigma^{\text{iso}}$  and inhomogeneous broadening  $\Delta\sigma$ . The latter two independent experimental measurables, i.e., the average position and the total width of the broadline, respectively, become overdetermined. We resolved this problem by applying external restrictions on the parameters from independent methods other than  $^{31}\text{P}$  broadline NMR simulations to determine unique values of the CS-tensor and ( $\alpha$ ,  $\beta$ ).

The values of the CS tensor components' (−81, −21, 108) ppm taken from experiments on bilayers (12) were adopted and varied simultaneously by “translation” of all the component values by adding or subtracting the same overall chemical shift to each component while the anisotropy of the original CS tensor was retained. An even more difficult problem, however, was the choice of the initial orientation ( $\alpha$ ,  $\beta$ ) of the CS tensor, for which there were no reliable data in the literature. The closest experimental reference was a single-crystal study involving phosphoryl-ethanolamine by Kohler and Klein (28). Among the most important results in that work is the determination of the orientation of the CS-tensor in the frame of the tetrahedral  $\text{PO}_4^{3-}$  moiety (Fig. 5), revealing the dominant role of the diamagnetic contribution to the P-nucleus chemical shift. The estimation of the rotation axis ( $\alpha$ ,  $\beta$ ) by Milburn and Jeffrey (29) using the interpretation of  $T_1$  measurements was the same as our estimation in our earlier work (20).

### Comparative studies

Our results concerning drug/membrane interactions using solid-state  $^{31}\text{P}$  NMR spectroscopy were compared with those from other physical chemical techniques, such as DSC,  $^{13}\text{C}$  NMR, and Raman spectroscopy.

### Differential scanning calorimetry

The phase-transition temperature of the DPPC bilayers with and without incorporation of losartan using variable concentrations has been studied (15,17). From these studies, it was

evident that the topography and the orientation of the drug molecule in the bilayer is strongly related to changes in the fluidity it causes.

In particular, DSC registered two endothermic phase transitions, the pretransition  $L_{\beta'}/P_{\beta'}$  and the main transition  $P_{\beta'}/L_{\alpha}$  in the DPPC bilayers. Incorporation of losartan in the bilayers for molar ratio equal to 5% or higher resulted in the abolishment of the pretransition because of severe perturbation at the hydrophilic-headgroup zone of the DPPC bilayers. Moreover, the incorporation of losartan resulted in lowering of the transition temperature  $T_m$  and an increase in the enthalpy change  $\Delta H$  (11), as well as in an increase in the half-height width of the main transition peak.

The DSC results are in agreement with those of the presented  $^{31}\text{P}$  NMR study, which detected strong hydrophilic interactions between losartan and the polar headgroup, leading to a significant upfield average shift and increased collective tilt by the incorporation of losartan.

### $^{13}\text{C}$ NMR spectroscopy

The losartan-loaded DPPC bilayers with molar ratio equal to 20% have been studied using  $^{13}\text{C}$  CP MAS (15). Increasing temperature resulted in increased mobility of the lipids leading to narrowing of the strong structureless peak at  $\sim 30$  ppm, which is attributed to the methylene ( $-\text{CH}_2-$ )<sub>10</sub> carbons. The presence of losartan caused decrease in the mobility of the ( $-\text{CH}_2-$ )<sub>10</sub> carbons and especially the terminal methyl group. Broadline  $^{31}\text{P}$  NMR simulations results also agree with the above findings. The interpretation of the brd profiles has led us to the conclusion that the mobility of the lipid molecules is partially hindered by the presence of losartan in the bilayers.

### Raman spectroscopy

Valuable information concerning the intramolecular interactions in the lipid molecules due to *trans/gauche* isomerism, as well as the intermolecular acyl-chain interactions of the lipids in the bilayers, can be retrieved through Raman spectroscopy. In particular, the relative intensity of certain peaks ( $2880\text{ cm}^{-1}$ ,  $2935\text{ cm}^{-1}$ ) depicts perturbations of the vibrational modes of the C-H bond as evidence of changes in the acyl chain, whereas the relative intensity of other peaks ( $1090\text{ cm}^{-1}$ ,  $1130\text{ cm}^{-1}$ ) is sensitive to intramolecular changes along the acyl chain, leading to a *trans/gauche* isomerization (30,31).

The Raman data acquired in this study were used to search for phase transitions on the basis of the inter- and intramolecular interactions. The temperature profile of the intensity ratio  $1090:1130\text{ cm}^{-1}$  (Fig. 10 a) shows that the inclusion of losartan in the bilayers hinders the lipid molecules from adopting *gauche* conformation in the liquid crystalline  $L_{\alpha}$  phase, indicating greater order with respect to unloaded bilayers. The profile of the intensity ratio  $2935:2880\text{ cm}^{-1}$  (Fig. 10 b), based on the effects of the intermolecular interactions on the

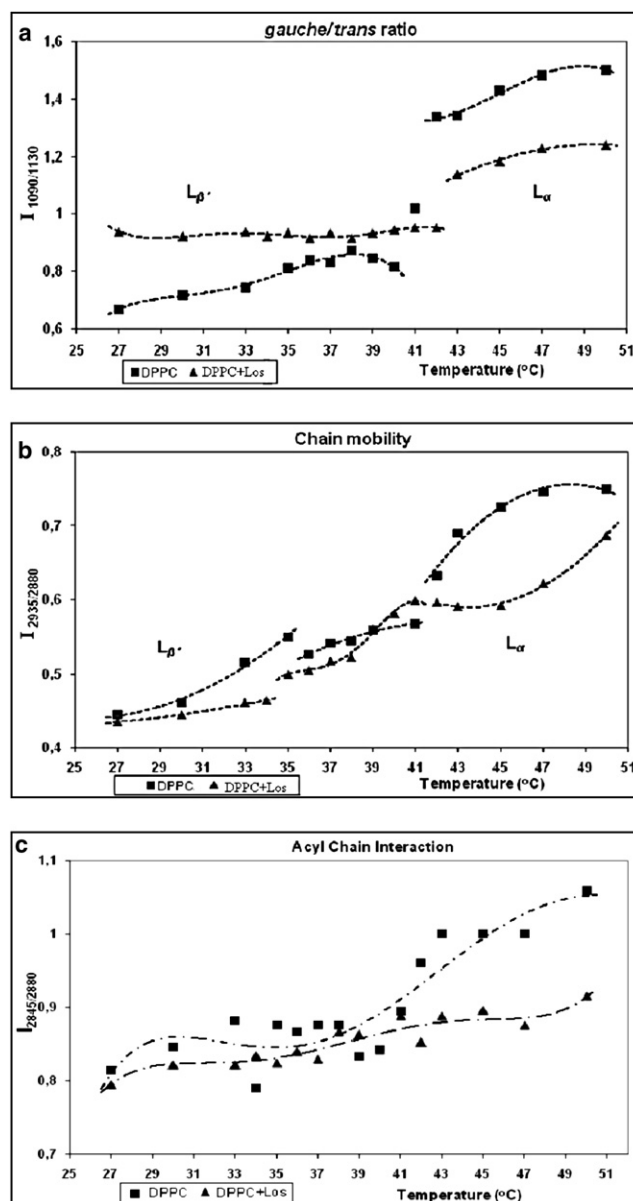


FIGURE 10 Experimental temperature profiles of Raman intensity ratios (a)  $1090:1130\text{ cm}^{-1}$ , (b)  $2935:2880\text{ cm}^{-1}$ , and (c)  $2850:2880\text{ cm}^{-1}$  for DPPC bilayers of the DPPC bilayers without and with losartan at a temperature range of  $27\text{--}50^\circ\text{C}$ .

Raman spectra, depicts decreased mobility of the hydrophobic alkyl chain of the lipids with the inclusion of losartan, compared to the mobility of the unloaded bilayers. The profile of  $2850:2880\text{ cm}^{-1}$  (Fig. 10 c) shows increased intermolecular interactions in the liquid crystalline phase between the acyl chains, interpreted as possible tail interdigitation (32,33). In addition, it was shown that the peak resonated at  $715\text{ cm}^{-1}$ , attributed to C-N stretching, in unloaded DPPC bilayers shifted from  $2$  to  $8\text{ cm}^{-1}$  when losartan was incorporated in the experimental range of temperatures. This is evidence of the strong electrostatic interactions between the



negatively charged pharmacophore segment of tetrazole and the positively charged choline group.

The above results are in agreement with the  $^{31}\text{P}$  NMR data. In particular, a close correspondence was observed in the abrupt change of the slope in the temperature profile of the intensity ratio  $1090:1130\text{ cm}^{-1}$  in the phase transition region with the  $\vartheta_{\text{DR}}$  and  $\Delta\sigma$  profiles of the  $^{31}\text{P}$  NMR simulation method.

## CONCLUSIONS

The presented, newly developed, quantitative broadband NMR spectral simulation methodology was applied on CP  $^{31}\text{P}$  NMR spectra of static samples of DPPC/H<sub>2</sub>O bilayers with and without the antihypertensive drug losartan. The simulations required fitting of several magnetic, dynamical, and structural parameters.

Evaluation of the temperature profiles of three out of a total of seven fitted parameters of the CP  $^{31}\text{P}$  NMR spectral simulations, the homogeneous broadening  $\text{brd}$ , the collective tilt  $\vartheta_{\text{DR}}$ , and the residual anisotropy  $\Delta\sigma$  gave significant information concerning conformation and dynamics of the bilayers. The temperature profiles of the fitted parameters for the two bilayer samples (drug-free DPPC or DPPC/losartan bilayers) were directly compared with each other, and the differences in the values of the parameters were related to the physicochemical disturbances of the bilayers by the losartan molecule. Two phase-transition temperatures were observed to be the result of sudden changes in the slope of the temperature profiles of mainly two parameters, the residual anisotropy  $\Delta\sigma$  and the collective tilt  $\vartheta_{\text{DR}}$ . The homogeneous broadening parameter  $\text{brd}$  reflecting the mobility of the individual lipid molecules was far less sensitive to the phase of the bilayer.

The application of the CP  $^{31}\text{P}$  NMR broadband simulations suggested that losartan was localized in the zone of the hydrophilic headgroup (34,35). Furthermore, losartan decreased the mobility of the lipid molecules, particularly the mobility of the alkyl chains, and increased the order of the bilayer. The information derived from the presented study is in agreement with the combined results obtained with DSC, Raman,  $^{13}\text{C}$ -MAS,  $^{31}\text{P}$  CP/MAS NMR, and EPR, all concluding that losartan anchors in the realm of the headgroup region (34,35).

Coauthors acknowledge the help of Dr. Joe Hayes for his useful contribution and of Prof. De-Ping Yang for his fruitful scientific discussions.

Research for this study was financed by the General Secretariat for Research and Technology of Greece through ENTER 04ER52. D.C. gratefully acknowledges financial support from the Alexander. S. Onassis Foundation.

## REFERENCES

1. Mavromoustakos, T., A. Kolocouris, M. Zervou, P. Roumelioti, J. Matsoukas, et al. 1999. An effort to understand the molecular basis of hypertension through the study of conformational analysis of

- losartan and sarmesin using a combination of nuclear magnetic resonance spectroscopy and theoretical calculations. *J. Med. Chem.* 42:1714–1722.
2. Zoumpoulakis, P., S. G. Grdadolnik, J. Matsoukas, and T. Mavromoustakos. 2002. Structure elucidation and conformational properties of eprosartan, a non peptide angiotensin II AT<sub>1</sub> antagonist. *J. Pharm. Biomed. Anal.* 28:125–135.
3. Zoumpoulakis, P., A. Zoga, P. Roumelioti, N. Giatas, S. G. Grdadolnik, et al. 2003. Conformational and biological studies for a pair of novel synthetic AT<sub>1</sub> antagonists. Stereoelectronic requirements for antihypertensive efficacy. *J. Pharm. Biomed. Anal.* 31:833–844.
4. Moutevelis-Minakakis, P., M. Gianni, H. Stougiannou, P. Zoumpoulakis, A. Zoga, et al. 2003. Design and synthesis of novel antihypertensive drugs. *Bioorg. Med. Chem. Lett.* 13:1737–1740.
5. Zoumpoulakis, P., A. Politi, S. G. Grdadolnik, J. Matsoukas, and T. Mavromoustakos. 2006. Structure elucidation and conformational study of V8. A novel synthetic non peptide AT<sub>1</sub> antagonist. *J. Pharm. Biomed. Anal.* 40:1097–1104.
6. Mavromoustakos, T., P. Moutevelis-Minakakis, C. G. Kokotos, P. Kontogianni, A. Politi, et al. 2006. Synthesis, binding studies, and in vivo biological evaluation of novel non-peptide antihypertensive analogs. *Bioorg. Med. Chem.* 14:4353–4360.
7. Benetis, N. P., I. Kyrikou, M. Zervou, and T. Mavromoustakos. 2005. Static  $^{31}\text{P}$  CP NMR multilamellar bilayer broadlines in the absence and presence of the Bioactive Dipeptide  $\beta$ -Ala-Tyr or Glu. *Chem. Phys.* 314:57–72.
8. Malcolm, I. C., Y. Z. Wu, and J. Higinbotham. 2003. The simulation of  $^{31}\text{P}$  NMR line shapes of lipid bilayers using an analytically soluble model. *Solid State Nucl. Magn. Reson.* 24:1–22.
9. Kohler, S. J., and M. P. Klein. 1977. Orientation and dynamics of phospholipid head group in bilayers and membranes determined from  $^{31}\text{P}$  nuclear magnetic resonance chemical shielding tensor. *Biochemistry.* 16:519–526.
10. Orådd, G., and G. Lindblom. 2004. Lateral diffusion studied by pulsed field gradient NMR on oriented lipid membranes. *Magn. Reson. Chem.* 42:123–131.
11. Houslay, M. D., and K. K. Stanley. 1982. Dynamics of Biological Membranes. John Wiley & Sons, New York.
12. Frye, J. A., B. S. Selinski, and P. L. Yeagle. 1985. Cross polarization  $^{31}\text{P}$  nuclear magnetic resonance of phospholipids. *Biophys. J.* 48:547–552.
13. De Casparo, M., K. J. Catt, T. Inagami, J. W. Wright, and T. Unger. 2000. International Union of Pharmacology. XXIII. The angiotensin II receptors. *Pharmacol. Rev.* 52:415–472.
14. Sakarellos, C., K. Lintner, F. Piriou, and S. Femandjian. 1983. Conformation of the central sequence of angiotensin II and analogues. *Biopolymers.* 22:663–687.
15. Zoumpoulakis, P., I. Daliani, M. Zervou, I. Kyrikou, E. Siapi, et al. 2003. Losartan's molecular basis of interaction with membranes and AT<sub>1</sub> receptor. *Chem. Phys. Lipids.* 125:13–25.
16. Matsoukas, J., G. Agelis, A. Wahhab, J. Hondrelis, D. Panagiotopoulos, et al. 1995. Differences in backbone structure between angiotensin II agonists and type I antagonists. *J. Med. Chem.* 38:4660–4669.
17. Theodoropoulou, E., and D. Marsh. 1999. Interactions of angiotensin II non-peptide AT<sub>1</sub> antagonist losartan with phospholipid membranes studied by combined use of differential scanning calorimetry and electron spin resonance spectroscopy. *Biochim. Biophys. Acta.* 1461:135–146.
18. Wen-guey, W., and C. Lang-Ming. 1990. Comparisons of lipid dynamics and packing in fully interdigitated monoarachidoyl-phosphatidylcholine and non-interdigitated dipalmitoyl phosphatidylcholine bilayers: cross polarization/magic angle spinning  $^{13}\text{C}$ -NMR studies. *Biochim. Biophys. Acta.* 1026:225–235.
19. Press, W. H., B. P. Flannery, S. A. Teukolsky, and W. T. Vetterling. Numerical Recipes. 1986. The Art of Scientific Computing. Cambridge University Press, Cambridge, UK.
20. Kyrikou, I., N.-P. Benetis, P. Chatzigeorgiou, M. Zervou, K. Viras, et al. 2008. Interactions of the dipeptide paralyisin  $\beta$ -Ala-Tyr and the

- aminoacid Glu with phospholipids bilayers. *Biochim. Biophys. Acta.* 1778:113–124.
21. Halle, B., and H. Wennerström. 1981. Interpretation of magnetic resonance data from water nuclei in heterogeneous systems. *J. Chem. Phys.* 75:1928–1943.
  22. Leach, A. R. 2001. *Molecular Modelling. Principles and Applications*, 2nd ed. Prentice-Hall, Harlow, England.
  23. Maswadeh, H., C. Demetzos, I. Daliani, I. Kyrikou, T. Mavromoustakos, et al. 2002. A molecular basis explanation of the dynamic and thermal effects of vinblastine sulfate upon dipalmitoylphosphatidylcholine bilayer membranes. *Biochim. Biophys. Acta.* 1567:49–55.
  24. Kyrikou, I., I. Daliani, T. Mavromoustakos, H. Maswadeh, C. Demetzos, et al. 2004. The modulation of thermal and dynamic properties of vinblastine by cholesterol in membrane bilayers. *Biochim. Biophys. Acta.* 1661:1–8.
  25. Dopico, A. M. 2007. *Methods in Membrane Lipids*. Humana Press.
  26. Gale, P., and A. Watts. 1992. Effect of bacteriorhodopsin on the orientation of the headgroup of 1, 2-dimyristoyl-sn-glycero-3-phosphocholine in bilayers: a  $^{31}\text{P}$ - and  $^2\text{H}$ -NMR study. *Biochim. Biophys. Acta.* 1106: 317–324.
  27. Lawson, K. D., and T. J. Flautt. 1967. Magnetically oriented lyotropic liquid crystalline phases. *J. Am. Chem. Soc.* 89:5489–5491.
  28. Kohler, S. J., and M. P. Klein. 1976.  $^{31}\text{P}$  Nuclear magnetic resonance chemical shielding tensor of phosphorylethanolamine, lecithin, and related compounds: application to head-group motion in modern membranes. *Biochemistry.* 15:967–973.
  29. Milburn, M. P., and K. R. Jeffrey. 1989. Dynamics of the phosphate group in phospholipid bilayers. A  $^{31}\text{P}$  angular dependent nuclear spin relaxation time study. *Biophys. J.* 56:543–549.
  30. Huang, C.-h., J. R. Lapidés, and I. W. Levin. 1982. Phase-transition Behavior of Saturated, Symmetric Chain Phospholipid Bilayer Dispersions Determined by Raman Spectroscopy: Correlation between Spectral and Thermodynamic Parameters. *J. Am. Chem. Soc.* 104:5926–5930.
  31. O' Leary, T. J., and I. W. Levin. 1984. Raman spectroscopic study of the melting behavior of anhydrous dipalmitoylphosphatidylcholine bilayers. *J. Phys. Chem.* 88:1790–1796.
  32. O' Leary, T. J., and I. W. Levin. 1984. Raman spectroscopic study of an interdigitated lipid bilayer dipalmitoylphosphatidylcholine dispersed in glycerol. *Biochim. Biophys. Acta.* 776:185–189.
  33. Hsu, J. C. Y., and C. M. Yip. 2007. Molecular dynamics simulations of indolicidin association with model lipid bilayers. *Biophys J. BioFAST.* L01–L03.
  34. Mavromoustakos, T., P. Zoumpoulakis, I. Kyrikou, A. Zoga, E. Siapi, et al. 2004. Efforts to understand molecular basis of hypertension through drug: membrane interactions. *Curr. Top. Med. Chem.* 4:445–459.
  35. Mavromoustakos, T., M. Zervou, P. Zoumpoulakis, I. Kyrikou, N. P. Benetis, et al. 2004. Conformation and bioactivity. design and discovery of novel antihypertensive drugs. *Curr. Top. Med. Chem.* 4:385–401.